Available online at www.sciencedirect.com
SCIENCE DIRECT®
Journal of Nuclear Materials 329–333 (2004) 652–656
journal of nuclear materials
www.elsevier.com/locate/jnucmat

Study on irradiation induced corrosion behavior in austenitic stainless steel using hydrogen-ion bombardment

Keietsu Kondou *, Akira Hasegawa, Katsunori Abe

Department of Quantum Science and Energy Engineering, Graduate School of Engineering, Tohoku University, 01 Aramaki-aza-Aoba, Aoba-ku, Sendai 980-8579, Japan

Abstract

In order to study the basic factors in irradiation assisted stress corrosion cracking (IASCC) of austenitic steels, the effects of displacement damage on the corrosion behavior of type 304 stainless steel were investigated by means of an ion irradiation technique. Solution-annealed specimens was irradiated using 1 MeV protons to 0.1, 0.5 and 1.0 dpa at about 573, 673 and 773 K. Electrochemical potentiokinetic reactivation (EPR) testing was carried out before and after the ion irradiation to clarify the effects of irradiation on corrosion behavior. The specimens irradiated at 773 K showed clear etching at grain boundaries and relatively high reactivation ratio, however, the specimens irradiated at 573 and 673 K showed no clear grain boundary etching. It was suggested that the higher irradiation temperature enhanced the radiation induced segregation near grain boundaries.

1. Introduction

Austenitic stainless steels have been used as structural materials in high temperature water and steam environments of nuclear power plants. Irradiation assisted stress corrosion cracking (IASCC) is one of the major issues for the integrity of water-cooled stainless steel core components in light water reactors [1]. To understand IASCC in austenitic steels will be useful also in the operation of fusion experimental reactor such as ITER. There are many important factors controlling IASCC, which relate to materials, stresses, environments and irradiation conditions. It is especially necessary to understand the role of irradiation on the change in corrosion and mechanical properties. Radiation induced segregation (RIS), including chromium depletion and nickel enrichment, is caused by neutron irradiation and is regarded as one of the controlling factors in IASCC. Ion irradiation can control precisely the experimental conditions such as temperature and dpa. It is useful to utilize hydrogen ion irradiation to study the fundamental behaviors of the change in mechanical properties [2] and corrosion properties in relation to the role of RIS in IASCC in stainless steel.

To estimate the effect of chromium depletion at grain boundaries on corrosion behavior, the electrochemical potentiokinetic reactivation (EPR) test is very useful. Katsura et al. applied this test to type 304 SS specimens irradiated in a BWR. They investigated the dependence on neutron fluence [3] and found that the irradiated specimens showed almost the same dependence of EPR properties on fluence as that indicated by IASCC susceptibility obtained through slow strain rate testing (SSRT). Therefore, it is interesting to study the influence of irradiation conditions on EPR properties. Light-ion irradiation can be used to simulate the effects of neutron irradiation, because it allows samples to be intentionally damaged to depths of 5–6 μm within a comparatively short time <12 h) and without radioactivation.

The purposes of this study are to clarify the actual corrosion behavior of irradiated samples using the EPR

* Corresponding author. Tel./fax: +81-22 217 7924.
E-mail address: kondou@jupiter.qse.tohoku.ac.jp (K. Kondou).

0022-3115/$ - see front matter © 2004 Elsevier B.V. All rights reserved.
doi:10.1016/j.jnucmat.2004.04.096

test method under controlled irradiation conditions, and to discuss the influence of temperature and dpa on corrosion resistance of austenite stainless steels.

2. Experimental

The test sample was type 304 stainless steel. The chemical composition of type 304 stainless steel were as follows, C: 0.06, Si: 0.57, Mn: 1.12, P: 0.032, S: 0.007, Ni: 8.66, Cr: 18.2, Fe: Bal. (in wt%). Disks of 3 mm in diameter and about 250 μm thick were punched out from 75% cold-worked stainless steel. The disks were solution annealed at 1223 K for 60 s in an evacuated quartz tube and water quenched after the heat treatment. The grain size of the heat-treated sample was about 20 μm. The specimen surface was mechanically polished and finally buffed to make a clean and flat surface. The specimen thickness after polishing was about 200 μm.

The ion-irradiation experiment was carried out using a Dynamitron accelerator at Tohoku University. Irradiation was conducted using 1 MeV proton. Fig. 1 shows the depth distribution of displacement damage calculated using TRIM code [4]. The damage was uniformly created from the irradiation surface to a depth of about 5 μm. Selected displacement damage levels in this area were 0.1, 0.5 and 1 dpa. The damage rate was 3.4×10^{-5} dpa/s, and specimen temperature during irradiation was 573, 673 and 773 K within an error of ±10 K, which was measured by an infrared pyrometer. These irradiation experiments were conducted in a vacuum of less than 5.0×10^{-6} Torr.

The electrochemical potentiokinetic reactivation (EPR) testing was carried out for ion-irradiated specimens and unirradiated sensitized specimens. Fig. 2 shows the schematic illustration of EPR test apparatus.

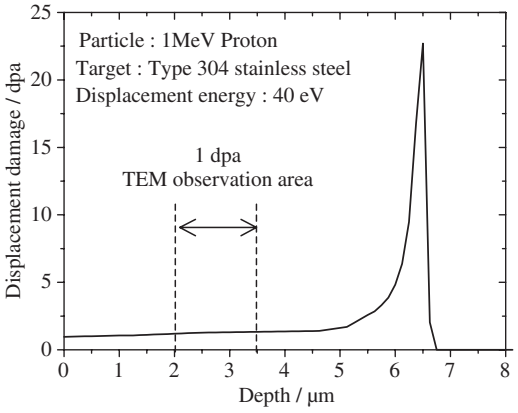

Fig. 1. Depth distribution of displacement damage in the case of 1 dpa specimen.

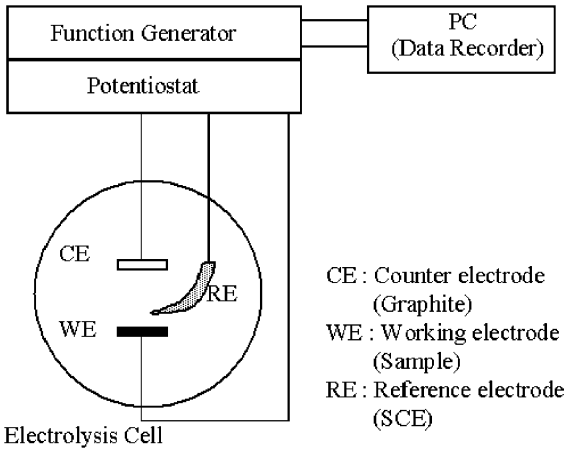

Fig. 2. Schematic of EPR test apparatus.

In order to estimate corrosion behavior, double-loop EPR (DL-EPR) testing was conducted in this work [3,5]. The DL-EPR testing was carried out in a test solution of 0.5 mol/l H_2SO_4 and 0.01 mol/l KSCN at about 303 ± 1 K, and a saturated calomel electrode (SCE) was used as a reference electrode. The potential sweep rate was 100 mV/min. The degree of sensitization was evaluated by the reactivation ratio (I_r/I_a), where I_a is the maximum anodic current and I_r is the maximum reactivation current. After EPR testing, a surface examination was performed using a JOEL JSM-5310LV scanning electron microscope (SEM). Transmission electron microscope (TEM) observation of hydrogen-ion irradiated conditions was conducted using a HITACH HF-2000 after electropolishing the irradiated specimens by combination of sectioning and backthinning.

3. Results and discussion

Fig. 3 summarizes EPR-tested surfaces of examined specimens, and the correlation between the reactivation ratio and irradiation dose is shown in Fig. 4. The surface of the unirradiated specimens after the EPR test was relatively flat (Fig. 3(a)). This result indicated the stable passive film formation on solution-annealed specimens, however, a thermally sensitized specimens showed significant etching at and around grain boundaries (Fig. 3(b)). The width of the etched area was about 5–6 μm on average. This preferential corrosion may have been caused by chromium depletion in the vicinity of the grain boundaries.

The surface micrographs after EPR tests of specimens irradiated at 573 K up to 0.1 and 1 dpa are shown in Fig. 3(c) and (d) respectively. Pitting, which could not be observed in the solution-annealed specimens, was observed. The surface pitting in the matrix might be

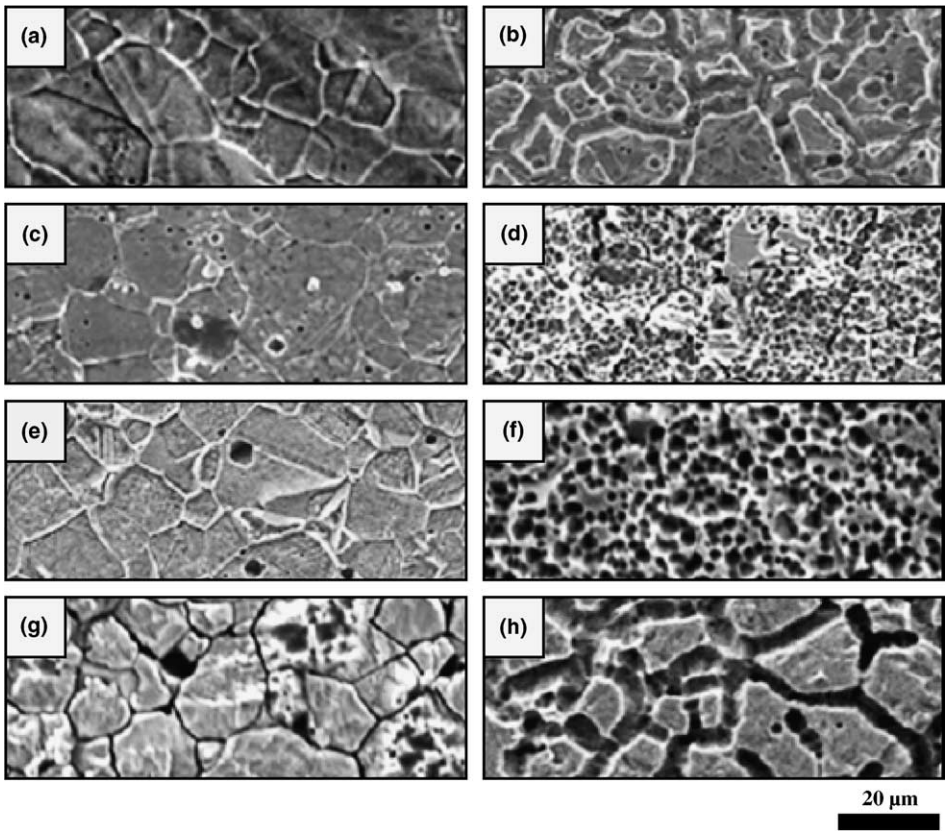

Fig. 3. SEM micrographs of post-EPR test on unirradiated and hydrogen-ion irradiated specimens. (a) solution-annealed specimen, (b) thermal sensitized at 923 K for 12 h, (c) and (d) irradiated at 573 K up to 0.1 and 1 dpa respectively, (e) and (f) irradiated at 673 K up to 0.1 and 1 dpa respectively, (g) and (h) irradiated at 773 K up to 0.1 and 1 dpa respectively.

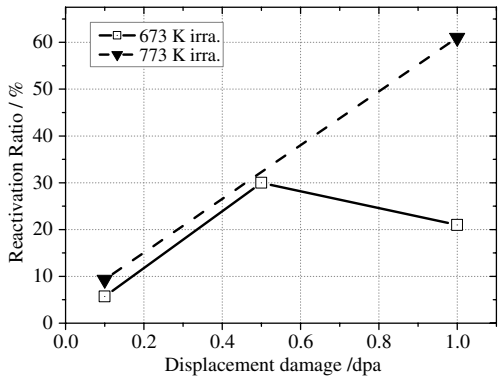

Fig. 4. Correlation between the reactivation ratio and displacement damage. Solid line: irradiated at 673 K, broken line: irradiated at 773 K.

attributed to irradiation, because this phenomenon was observed only in irradiated specimens and the number of pits increased with irradiation dose. No clear etching trenches along grain boundaries are observed in Fig. 3(c). Fine etching trenches along grain boundaries are observed in Fig. 3(d), but it is difficult to distinguish whether they are the sequence of pits or the dissolution associated with RIS. Dewi et al. reported that chromium concentration at grain boundaries of 304SS decreased from 18.5 to 13.5 wt% after hydrogen ion irradiation at 573 K up to 1 dpa [6]. Fig. 3(e) and (f) show surface micrographs of the EPR tested specimens irradiated at 673 K up to 0.1 and 1 dpa respectively. The corrosion behavior of specimens irradiated at 673 K was similar to that of specimens irradiated at 573 K. Although RIS occurred in proton-irradiated specimens, the stability of the passive film at and around grain boundaries seemed to be maintained.

Specimens irradiated at 773 K showed different corrosion behavior in this EPR testing condition than that of specimens irradiated at 573 or 673 K. Surface micrographs obtained after the EPR testing of specimens irradiated at 773 K up to 0.1 and 1 dpa are shown in Fig. 3(g) and (h) respectively. The micrographs show

the dissolution of the passive film at and around the grain boundaries, and the dissolution width increases with the irradiation dose. As shown in Fig. 4 later, the reactivation ratio of those specimens also increases with dose. These results indicate a correlation between the dissolution volume and the reactivation ratio. On the other hand, the surface pitting after EPR testing which was observed in the specimens irradiated at 573 and 673 K was not observed in specimens irradiated at 773 K. To clarify whether there was a effect of thermal sensitization or not, EPR testing on the unirradiated specimen annealed at 773 K for 8 h was conducted. In this case, the reactivation ratio was 0.5%, and this indicated little effect of thermal sensitization in the specimens irradiated at 773 K. Thus, the reactivation ratio obtained in EPR testing on specimens irradiated at 773 K indicates chemical activation at and around grain boundaries induced by proton irradiation. One of the causes of the chemical activation might be RIS after 773 K irradiation, i.e. more chromium depletion or a wider depleted area after higher temperature irradiation. To clarify the conditions in which etching trenches along grain boundaries can be observed in EPR testing, further investigation on RIS of specimens irradiated at 773 K is required.

It is reported that the width of the chromium depleted region by electron irradiation at 623 K is about 30 nm [7], and thus the width of RIS after irradiation at 773 K may be larger than 30 nm. In Fig. 3(g), the width of the etched area at grain boundaries is 4–5 μm, and this value is much larger than the presumed width of chromium depleted region. It is possible that once the passive film in the chromium depleted region at the grain boundaries break down, dissolution occurs not only in the chromium depleted region but also in the vicinity of that region due to chemical activation at grain boundaries such as edge effects.

Fig. 4 shows the correlation between reactivation ratio and dpa after 673 and 773 K irradiation. The reactivation ratio of specimens irradiated at 773 K increased with dose, though that of specimens irradiated at 673 K saturated at higher dose. The ratios are relatively large compared with those obtained after neutron irradiation at 561 K [3]. The reasons why the ratios in the present results are larger than neutron irradiation condition are due to severe pitting in the matrix in the case of 673 K irradiation, and grain boundary etching in the case of 773 K irradiation respectively.

Typical microstructures of specimens irradiated up to 0.1 dpa at 673 and 773 K are shown in Fig. 5(a) and (b) respectively. Irradiation defects such as faulted loops and black dots were observed. The defect density tends to decrease with irradiation temperature, i.e. about $1.5\times10^{21}/m^2$ in the specimens irradiated at 673 K, $1.1\times10^{20}/m^2$ in those at 773 K. Cavities were not observed. It is known that the passive film of unirradiated

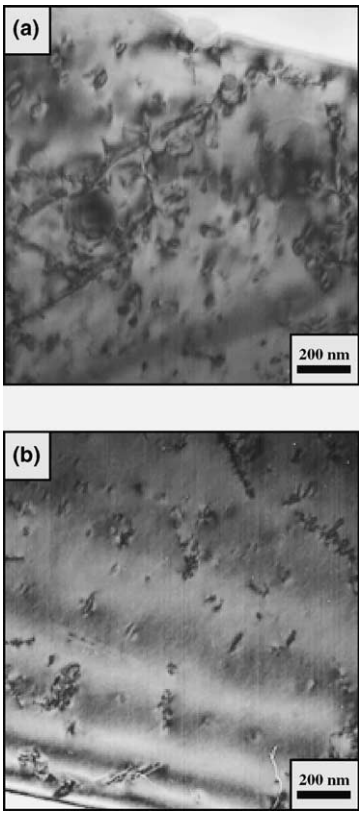

Fig. 5. TEM micrographs of the specimens after irradiation up to 0.1 dpa: (a) 673 K and (b) 773 K.

thermal sensitized specimens near grain boundaries dissolves in the EPR test (Fig. 3(b)) due to chromium depletion resulting from the formation of chromium carbide. On the other hand, the large precipitations induced by the irradiation were not observed, nevertheless pitting in the matrix in 673 K irradiated specimens and etching near grain boundaries in 773 K irradiated specimens were observed. TEM/EDS analysis showed the degree of grain boundary segregation detected after 773 K irradiation was larger than that after 573 or 673 K irradiation. The details of RIS results related to corrosion behavior will be presented elsewhere.

Whether the grain boundaries or the matrix is chemically attacked may be determined by the balance between the degree of RIS at grain boundaries and the damage density in the matrix. It is suggested that in specimens irradiated at 573 or 673 K, small RIS near grain boundaries and a high density of irradiation damage defects leads to reduced grain boundary etching and clear pitting in the matrix. On the other hand, in the specimens irradiated at 773 K, larger RIS near grain boundaries and the recovery of irradiation damage due to high temperature irradiation lead to clear grain boundary etching and little pitting in the matrix.

4. Summary

The corrosion behavior of solution-annealed and proton-irradiated type 304 austenitic stainless steel was investigated using EPR testing after irradiation at 573, 673 and 773 K up to 0.1 and 1 dpa. The results are summarized as follows:

1. In the specimens irradiated at 573 and 673 K, surface pitting was observed after EPR testing and the number density of pits increased with irradiation dose. No grain boundary etching trench was observed. In the specimens irradiated at 773 K, etching trenches at and around grain boundaries were observed, and surface pitting was not observed.
2. The reactivation ratio of specimens irradiated at 773 K increased with dose, though that of specimens irradiated at 673 K saturated at higher dose.
3. It is suggested that in specimens irradiated at 573 or 673 K, small RIS near grain boundaries and many irradiation damage lead to no grain boundary etching and pitting in the matrix. On the other hand, in the specimens irradiated at 773 K, larger RIS near grain boundaries and the recovery of irradiation damage due to high temperature irradiation lead to clear grain boundary etching and less pitting in the matrix.

Acknowledgements

We would like to express our thanks to Messers S. Matsuyama, R. Sakamoto and M. Fujisawa, staff at Fast Neutron Laboratory at Tohoku University, for their help with accelerator experiments. We are also thankful to Dr V. Kain, research staff at Tohoku University, for his advice on EPR tests.

References

[1] S.M. Brummer, J. Nucl. Mater. 216 (1994) 348.
[2] G.S. Was, J.T. Busby, T. Allen, E.A. Kenik, A. Jenssen, S.M. Buruemmer, J. Gan, A.D. Edwards, P.M. Scott, P.L. Andressen, J. Nucl. Mater. 300 (2002) 198.
[3] R. Katsura, M. Kodama, S. Nishimura, Corrosion 48 (1992) 384.
[4] J.P. Biersack, J. F. Ziegler, TRIM85 Program, IBM Corp. Yorktown, NY, 1985.
[5] G.E.C. Bell, T. Inazumi, E.A. Kenik, T. Kondo, J. Nucl. Mater. 187 (1992) 170.
[6] K. Dewi, A. Hasegawa, S. Otsuka, K. Abe, Fus. Technol. 39 (2001) 585.
[7] S. Watanabe, N. Sakaguchi, S. Mochizuki, H. Takahashi, J. Nucl. Mater. 271&272 (1999) 184.